Available online at www.sciencedirect.com
SCIENCE DIRECT®
International Journal of Thermal Sciences 45 (2006) 586–594
International Journal of Thermal Sciences
www.elsevier.com/locate/ijts

A numerical study of laminar methane/air triple flames in two-dimensional mixing layers

Hongsheng Guo *, Fengshan Liu, Gregory J. Smallwood

Combustion Research Group, Institute for Chemical Process and Environmental Technology, National Research Council of Canada, Building M-9, 1200 Montreal Road, Ottawa, ON, Canada K1A 0R6

Received 22 March 2005; received in revised form 30 June 2005; accepted 2 August 2005

Available online 6 October 2005

Abstract

Triple flames formed in methane/air mixing layers with three different mixture fraction gradients were investigated by numerical simulation. The primitive variable method, in which the fully elliptic governing equations were solved with detailed chemistry and complex thermal and transport properties, was used. Radiation heat transfer from CO_2, CO and H_2O was calculated using the discrete-ordinates method coupled to a statistical narrow band correlated-K based wide band model. The results show that with the increase of the mixture fraction gradient, the combustion intensity in the diffusion flame branch of a triple flame is enhanced. In the near-stoichiometric mixture fraction region, the local burning flux of a triple flame is reduced when the mixture fraction gradient is increased. However, when the mixture fraction is significantly different from the stoichiometric value, the local burning flux increases as the mixture fraction gradient is increased. The correlation of the burning speed versus stretch rate established from conventional homogeneous premixed flames cannot completely explain the phenomena observed in triple flames. The interaction between the diffusion and premixed flame branches significantly affects the local burning velocity in regions where the mixture fraction is far from the stoichiometric value in a triple flame. This interaction is caused by both conduction heat transfer and radical exchange. Radiation has negligible effect on local burning properties in a triple flame.

Keywords: Laminar flame; Triple flame; Premixed flame; Radiation; Stratified combustion

1. Introduction

A triple flame is usually formed in a partially premixed mixture. Triple flames were first observed by Phillips [1] in an experimental study of a methane/air mixing layer in 1965. The problem was later addressed analytically by Liñán and Crespo [2] using large activation energy asymptotics in 1976. This approach was extended by Dold [3] to include the upstream heat conduction. Using a similar model, Kĩoni et al. [4] studied the response of the structure and propagation velocity of a triple flame to the strain in a counterflow configuration by a simplified numerical model. Since then many researchers have extensively studied this issue from various viewpoints. Ruetsch et al. [5] and Boulanger et al. [6] studied the effect of heat release on triple flames. The structure and propagation of methanol/air and methane/air triple flames in 2-D mixing layers were numerically studied respectively by Echekki and Chen [7] and Kĩoni et al. [8]. Buckmaster and Matalon [9] studied the effects of Lewis number on triple flames. Azzoni et al. [10] investigated the effect of gravity on triple flames. Plessing et al. [11] experimentally and numerically studied the structure and propagation of triple flames produced by an axisymmetric co-flow burner with a central diluted fuel jet and a surrounding fuel co-flow; a reduced chemistry was used in the simulations. Qin et al. [12] also studied the characteristics of lifted triple flames stabilized in the near field of a partially premixed axisymmetric jet. Im and Chen [13,14] studied triple flames in partially premixed hydrogen-air mixtures and the effects of flow strain on triple flame propagation by direct numerical simulation and detailed chemistry. Lockett et al. [15] experimentally examined the structure and stability of laminar counterflow triple flames. Ko and Chung [16] and Lee et al. [17] experimentally studied the propagation of unsteady triple flames in laminar non-premixed jets. The

* Corresponding author. Tel.: +1 613 991 0869; fax: +1 613 957 7869.
E-mail address: hongsheng.guo@nrc-cnrc.gc.ca (H. Guo).

1290-0729/$ – see front matter
doi:10.1016/j.ijthermalsci.2005.08.010

propagation of triple (edge) flames produced by opposed jets were experimentally and numerically investigated respectively by Santoro et al. [18] and Frouzakis et al. [19].

Most previous studies on triple flames focused on the propagation of the triple point. Due to the variation in equivalence ratio along the flame front and the co-existence of the three flame branches, it is interesting to examine the local burning speed along the entire front of a triple flame. The characteristics of local burning speed along the front of a triple flame significantly affect the combustion and formation of pollutant, such as NO_X, in a partially premixed mixture. In spite of the importance of this property, only Plessing et al. [11] and Qin et al. [12] provided the details of the local burning velocity distribution in a triple flame. While Qin et al. [12] indicated that like in a premixed flame, there is a good correlation between the stretch rate, Lewis number, and flame propagation speed in both the rich and the lean premixed zones, Plessing et al. [11] showed that such a simple correlation does not exist for a triple flame. Moreover, Refs. [11,12] each studied the local burning speed for only one triple flame. To our knowledge, no study on the effect of mixture fraction gradient, the most significant parameter affecting the propagation characteristics of a triple flame, on local burning speed along the entire flame surface of a triple flame has ever been reported.

In this paper, three triple flames with different mixture fraction gradients in two dimensional methane/air mixing layers are numerically investigated. The local propagation speed along the flame front of a triple flame and the effect of mixture fraction gradient will be examined and discussed. For the purpose of presentation, the structures of triple flames and the effect of mixture fraction gradient are first briefly discussed.

2. Flame configuration and numerical method

The simulation was carried out in a 3 cm (x) × 5 cm (y) two-dimensional rectangular domain, as shown in Fig. 1. The fresh methane/air mixture enters the domain from the bottom at atmospheric pressure, with the velocity and temperature being 50 cm·s^{-1} and 298 K, respectively. The equivalence ratio (ϕ) at the inlet linearly varies from 0.0 to 2.0 within a mixing layer. Then a triple flame is expected to form inside the domain.

Methane/air triple flames with three different mixture fraction gradients, obtained by using the mixing layer thickness (L_m) of 0.5, 1.0 and 2.0 cm, respectively, were studied.

The numerical model solved fully elliptic governing equations for the conservation of mass, momentum, energy and chemical species. The governing equations are [20]

Continuity:

$$\frac{\partial}{\partial x}(\rho u)+\frac{\partial}{\partial y}(\rho v)=0 \tag{1}$$

Momentum:

$$\rho u\frac{\partial u}{\partial x}+\rho v\frac{\partial u}{\partial y} =-\frac{\partial p}{\partial x}+2\frac{\partial}{\partial x}\left(\mu\frac{\partial u}{\partial x}\right)+\frac{\partial}{\partial y}\left(\mu\frac{\partial u}{\partial y}\right) -\frac{2}{3}\frac{\partial}{\partial x}\left(\mu\frac{\partial u}{\partial x}\right)-\frac{2}{3}\frac{\partial}{\partial x}\left(\mu\frac{\partial v}{\partial y}\right)+\frac{\partial}{\partial y}\left(\mu\frac{\partial v}{\partial x}\right) \tag{2}$$

$$\rho u\frac{\partial v}{\partial x}+\rho v\frac{\partial v}{\partial y} =-\frac{\partial p}{\partial y}+2\frac{\partial}{\partial y}\left(\mu\frac{\partial v}{\partial y}\right)+\frac{\partial}{\partial x}\left(\mu\frac{\partial v}{\partial x}\right) -\frac{2}{3}\frac{\partial}{\partial y}\left(\mu\frac{\partial u}{\partial x}\right)-\frac{2}{3}\frac{\partial}{\partial y}\left(\mu\frac{\partial v}{\partial y}\right)+\frac{\partial}{\partial x}\left(\mu\frac{\partial u}{\partial y}\right)-\rho g \tag{3}$$

Energy:

$$c_p\left(\rho u\frac{\partial T}{\partial x}+\rho v\frac{\partial T}{\partial y}\right)=\frac{\partial}{\partial x}\left(\lambda\frac{\partial T}{\partial x}\right)+\frac{\partial}{\partial y}\left(\lambda\frac{\partial T}{\partial y}\right) -\sum_{k=1}^{KK}\left[\rho c_{pk}Y_k\left(V_{kx}\frac{\partial T}{\partial x}+V_{ky}\frac{\partial T}{\partial y}\right)\right] -\sum_{k=1}^{KK}h_kW_k\omega_k+q_r \tag{4}$$

Chemical species:

$$\rho u\frac{\partial Y_k}{\partial x}+\rho v\frac{\partial Y_k}{\partial y}=-\frac{\partial}{\partial x}(\rho Y_kV_{kx})-\frac{\partial}{\partial y}(\rho Y_kV_{ky})+W_k\omega_k \quad k=1,2,\ldots,KK \tag{5}$$

where u and v are the velocities in x and y directions, respectively; T the temperature of the mixture; ρ the density of the mixture; W_k the molecular weight of the kth species; λ the mixture thermal conductivity; c_p specific heat of the mixture under constant pressure; c_{pk} specific heat of the kth species under constant pressure; ω_k mole production rate of the kth species per unit volume. Quantity h_k denotes the specific enthalpy of the kth species; g the gravitational acceleration which was in

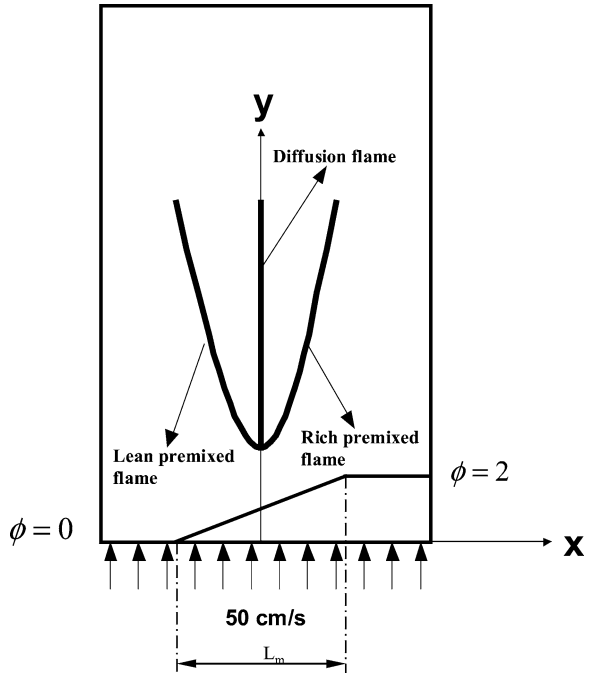

Fig. 1. Computational configuration.

the vertical (y) direction; μ the viscosity of the mixture; Y_k the mass fraction of the kth species; V_{kx} and V_{ky} the diffusion velocities of the kth species in x and y directions; and KK the total species number. The set of governing equations was closed by the ideal gas state equation.

The last term on the right-hand side of Eq. (4), q_r, is the source term due to radiation heat transfer. It was obtained by the discrete ordinate method coupled to a statistical narrow-band correlated-K (SNBCK) based wide band model for the properties of CO, CO_2 and H_2O [21].

The species diffusion velocity consists of three terms: ordinary diffusion, thermal diffusion and correction diffusion velocities, i.e.

$$V_{kx_i} = V_{okx_i} + V_{Tkx_i} + V_{cx_i}$$
$$k = 1, 2, \ldots, KK, \quad x_i = x, y \tag{6}$$

The ordinary diffusion velocity, V_{okx_i}, and the thermal diffusion velocity, V_{Tkx_i}, were respectively calculated by the approximate mixture-average formulation and the accurate multicomponent formulation [22]. The correction diffusion velocity, V_{cx_i}, was introduced to ensure the net diffusive flux of all species to be zero.

Low Mach number flow was assumed, and hence the pressure difference only affects the velocity field. The governing equations were discretized using the control volume method. The SIMPLE numerical scheme [23] was used to deal with the pressure and velocity coupling. The diffusion and convective terms in the conservation equations were respectively discretized by the central and upwind difference methods. A 260×232 cell mesh was used, with finer uniform grid in the triple region (the common region of origin of the three flame branches), where the grid size was 0.0625×0.0625 mm^2. It has been checked that the further refinement of grid does not significantly affect the result. The discretized equations of species mass fraction were solved simultaneously for every cell to accelerate the convergence process [24], while those of momentum, energy and pressure correction were solved sequentially using the tri-diagonal matrix algorithm (TDMA).

The free slip boundary condition was used for the left- and right-hand side boundaries, and zero gradient condition was used for the outlet (the upper boundary). The inlet velocity and temperature were fixed as 50 cm·s^{-1} and 298 K, respectively. The species concentrations at the inlet were specified according to the local equivalence ratio.

The chemical reaction mechanism used is essentially from GRI-Mech 3.0 [25], with the removal of the reactions and species related to NO_X formation (except N_2). The revised reaction scheme consists of 36 species and 219 reactions. The thermal and transport properties were obtained by using the database of GRI-Mech 3.0 and the algorithms given in [22,26].

3. Results and discussion

3.1. Structure of triple flames

The above described flame configuration and three mixing layers formed three linear mixture fraction profiles, with mixture fraction gradients being, respectively, 0.208, 0.104 and 0.052 cm^{-1}, corresponding to the mixing layer thicknesses of 0.5, 1.0 and 2.0 cm. Mixture fraction was calculated by the definition in [27].

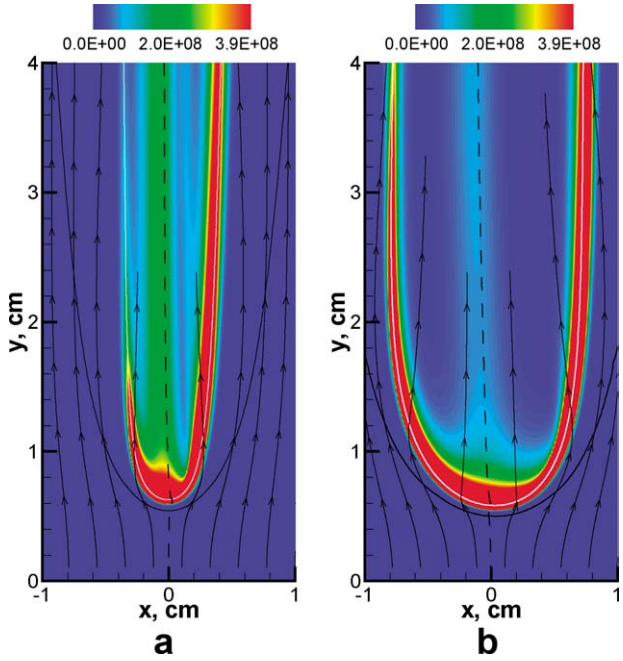

Fig. 2. Heat release rate, erg·cm^{-3}s^{-1}. (a) $L_m = 0.5$ cm; (b) $L_m = 2.0$ cm. Dashed line represents the position of the stoichiometric mixture fraction.

Fig. 2 shows the heat release rate distributions, streamlines and two contour lines for two triple flames with mixing layer thickness (L_m) of 0.5 and 2.0 cm. Results of the flame with L_m of 1.0 cm are qualitatively similar, but quantitatively between those of $L_m = 0.5$ and 2.0 cm. To save space, the results for the flame with L_m of 1.0 cm are not shown in Figs. 2–4. The black dashed line represents the position of the stoichiometric mixture fraction (0.055). The black and white solid lines are respectively the contour lines with temperature of 300 K and CO_2 mole fraction (X_{CO_2}) of 0.043. The lines with arrows are the streamlines. The structure of triple flames is clearly illustrated. There are three main heat release branches for each flame. To the left and right are the lean and rich premixed flame branches, respectively. Between them, there is a diffusion flame branch formed along the line of stoichiometric mixture fraction. Hereafter the three flame branches are also referred to as the lean, the rich and the diffusion flames/branches. They have a common region of origin, known as the triple region. The flow diverges ahead of the triple region due to heat expansion [5], which is the reason that a triple flame can be self-stabilized in an environment with a higher upstream speed.

The heat release rate in the diffusion flame is much lower than in the premixed flames. Comparing the two triple flames, it is observed that the heat release rate in the diffusion branch of the triple flame with the narrower mixing layer is higher than that with the wider mixing layer. Since the mixture fractions (equivalence ratios) on the two sides of the mixing layers were same for all the studied triple flames, narrower mixing layer means higher mixture fraction gradient. This implies that the

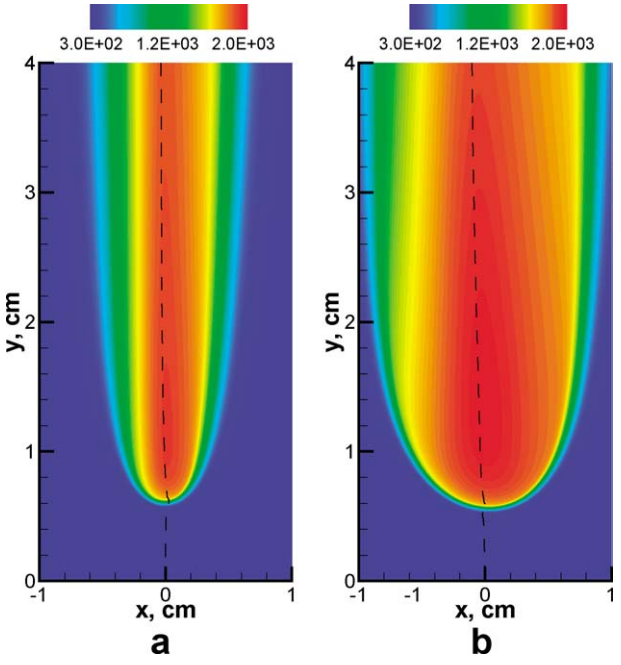

Fig. 3. Flame temperature, K. (a) $L_m = 0.5$ cm; (b) $L_m = 2.0$ cm. Dashed line represents the position of the stoichiometric mixture fraction.

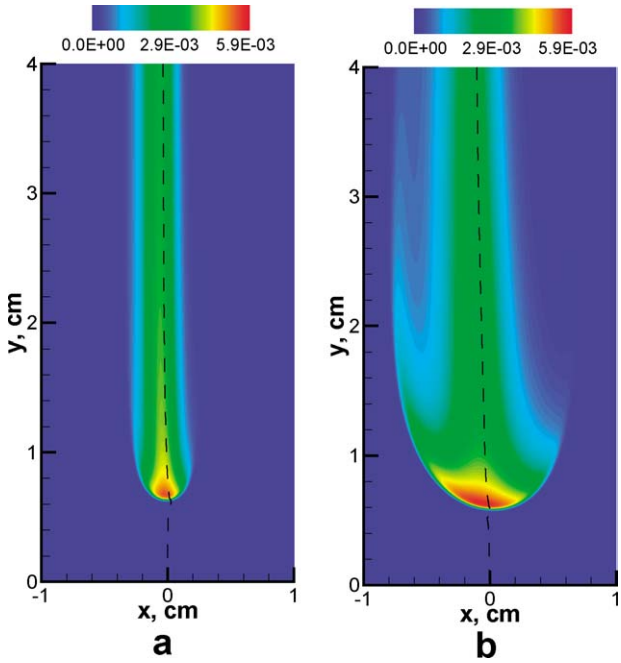

Fig. 4. Mole fraction of OH. (a) $L_m = 0.5$ cm; (b) $L_m = 2.0$ cm. Dashed line represents the position of the stoichiometric mixture fraction.

combustion intensity is higher in the diffusion flame when the upstream mixture fraction gradient is increased. Such a result is consistent with the theoretical analysis in [3].

Shown in Fig. 3 are the flame temperature distributions for the two triple flames described above. It is indicated that the temperature peaks around the stoichiometric line in a triple flame. This is because the excess burning components (mainly CO and H_2 formed in the rich branch) and oxygen (from the lean branch) further react in the diffusion flame. As a result, there should be lateral heat transfer from the diffusion flame to the premixed flames due to conduction and radiation. This causes the burning speeds and the flammability limits of the premixed flames to differ from those of the corresponding one-dimensional planar lean and rich premixed flames, as discussed later.

Fig. 4 displays the distributions of OH mole fraction for the two triple flames. The concentration of OH peaks in the triple region for both flames. Among the three branches of each triple flame, the concentration of OH in the diffusion flame is higher than in the two premixed flames. For the flame with $L_m = 2.0$ cm, the OH distribution shows three higher concentration regions, corresponding to the three flame branches. In the regions between the diffusion flame and the two premixed flames, the concentration of OH is lower. However, the situation in the flame of $L_m = 0.5$ cm varies. The three flame branches are very close, and there are no regions of significantly low OH concentration between the diffusion and the premixed flames. Although not shown, other radicals, like H, have the similar phenomenon. This is because the distances between the diffusion flame and the two premixed flames decrease with the reduction in the mixing layer thickness, and the burning intensity in the diffusion flame relatively increases. As a result, the interaction between the diffusion flame and the two premixed flames is intensified when the mixing layer is narrower. More radicals produced in the diffusion flame, such as OH and H, can diffuse to the premixed branches in triple flames of narrower mixing layer. This radical diffusion can enhance the fuel decomposition and combustion in the two premixed flames. This is very important, since the local burning velocities along the two premixed flames will be more significantly affected by the diffusion branch in triple flames of narrower mixing layer, as discussed in the next section.

The concentrations of the primary fuel (CH_4), oxygen (O_2), and two intermediate species H_2 and CO for the flame of $L_m = 2.0$ cm are shown in Fig. 5. The other two flames have qualitatively similar results. It is revealed that no primary fuel (CH_4) can reach the diffusion flame, while excess oxygen can penetrate the lean premixed flame and reach the diffusion flame. In the rich premixed flame, the primary fuel is converted to some intermediate species, such as H_2 and CO, and these intermediate species are consumed in the diffusion flame. These results are consistent with the observation in [7] for methanol/air triple flames.

3.2. *Local burning flux along the flame surface*

Due to the variation in equivalence ratio, an interesting property of triple flames is the local burning flux, the product of local flame propagation speed and density, along the flame surface. There are multiple definitions for flame speed. Although some researchers argued that the consumption speed is more meaningful to represent the burning velocity [28], the local value is difficult to obtain for multi-dimensional flames. Like other studies [12,13], the displacement speed is used in this paper. Generally it can be obtained by equating the transport equation for a scalar variable with the Hamilton–Jacobi equation for the

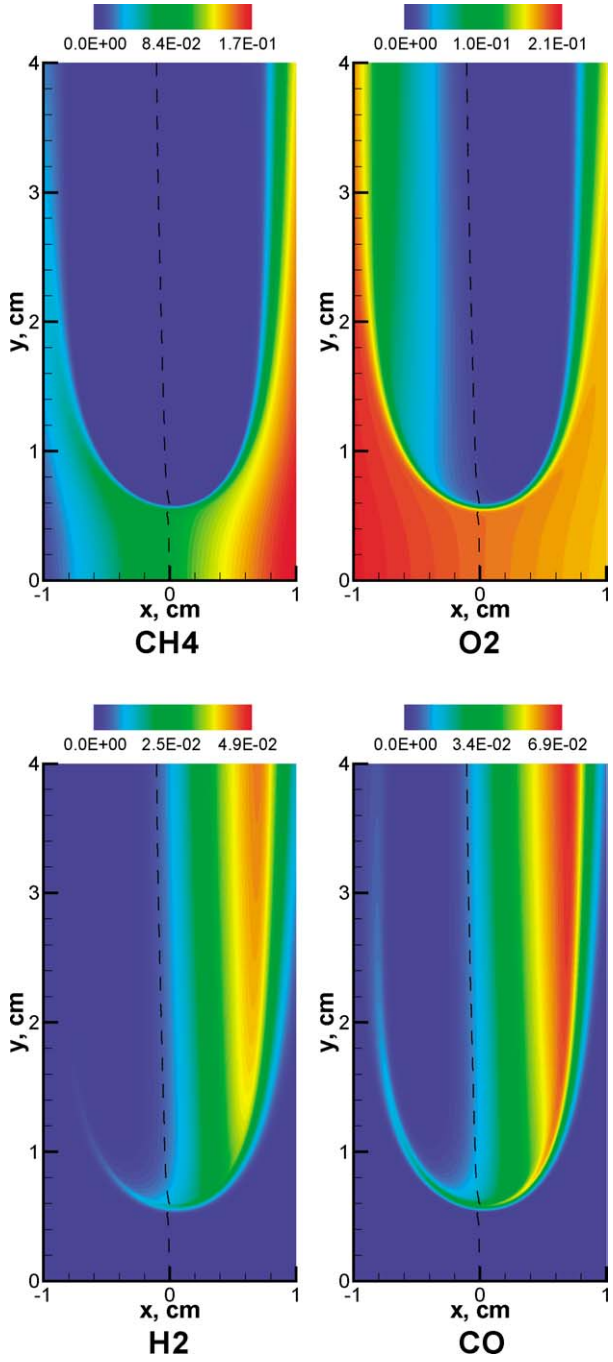

Fig. 5. Mole fractions of CH_4, O_2, H_2 and CO for the flame of $L_m = 2.0$ cm. Dashed line represents the position of the stoichiometric mixture fraction.

scalar field [5]. For a steady state simulation, this property can be simply obtained by evaluating the local fluid velocity normal to the flame surface.

A difficulty in calculating the displacement speed is to locate the flame surface. As a flame has a finite thickness, there is some ambiguity in selecting this surface. In the previous studies [12,13], the contour line with a constant OH or H_2O mass fraction was selected. However neither was found to properly represent the envelopes of the triple flames investigated in this study. Alternatively the contour line with the CO_2 mole fraction of 0.043, the white solid line in Fig. 2, was found to reasonably represent the envelopes of the current triple flames. This choice is a best fit to the reaction surfaces of the premixed flame branches. The stream tube area varies across the flame due to the flow divergence, which usually causes the variation in burning flux along a stream tube. In order to examine this variation and obtain the common feature of the local burning velocity in a triple flame, in addition to the contour line of $X_{CO_2} = 0.043$, the contour line of $T = 300$ K (the black solid line in Fig. 2) was also used to evaluate the local burning flux. The former is the reaction surface of the premixed flame branches of a triple flame, whereas the latter represents the flame front (upstream) surface. We chose the burning flux, rather than the speed, to reflect the burning intensity, since it is affected mainly by the variation of the stream tube area, while the speed is affected by the variations in both the stream tube area and the temperature.

Fig. 6 shows the local burning flux versus mixture fraction [27] obtained from the two surfaces for the three triple flames. The data for one-dimensional planar CH_4/air premixed flames, obtained from the web site of GRI—Mech 3.0 [25], are also shown for comparison. Note that the burning flux of a one-dimensional planar premixed flame is constant along the whole flame layer. From this figure, it is first observed that the burning fluxes for the two surfaces are significantly different. For a given mixture fraction, the burning flux from the contour line of $T = 300$ K is greater than that from the contour line of $X_{CO_2} = 0.043$. This is caused by the variation in the stream tube area across the flame, which is similar to a premixed flame with a varying stream tube area, like an inwardly—or outwardly-propagating flame [29], and the preferential diffusion. Compared to the burning flux from the contour line of $X_{CO_2} = 0.043$, the differences in the local burning fluxes of the three studied triple flames obtained from the contour line of $T = 300$ K decrease in the near-stoichiometric mixture fraction (0.055) region, and increase in the region where the mixture fraction is far from the stoichiometric value.

Secondly, we note from Fig. 6 that the local burning flux along a flame surface of a triple flame is apparently lower than that of the corresponding one-dimensional planar flame when the mixture fraction is near the stoichiometric value. In spite of the quantitative difference in the burning fluxes obtained from the two surfaces, there is a common feature. The narrower the mixing layer, the lower the burning flux in the near-stoichiometric mixture fraction region. A one-dimensional premixed flame can be seen as a triple flame formed in an infinitely wide mixing layer. However, as the mixture fraction is varied from the stoichiometric value, for both the rich and the lean directions, the difference in the burning fluxes between the 1-D premixed flame and the triple flames gradually decreases, and eventually the effect of the mixing layer thickness on burning flux reverses. This is a feature of triple flames. When the mixture fraction is far from the stoichiometric value, the burning flux obtained from the contour line of $T = 300$ K is higher than that of the 1-D planar premixed flame. In the following paragraphs, we will discuss this common feature of local burning flux in triple flames mainly based on the results from the contour line of $X_{CO_2} = 0.043$, since they represent the burning speed of the premixed flame branches of a triple flame and

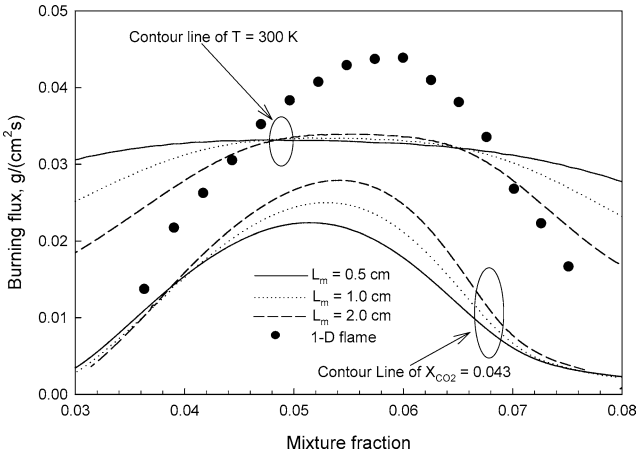

Fig. 6. Local burning flux versus mixture fraction.

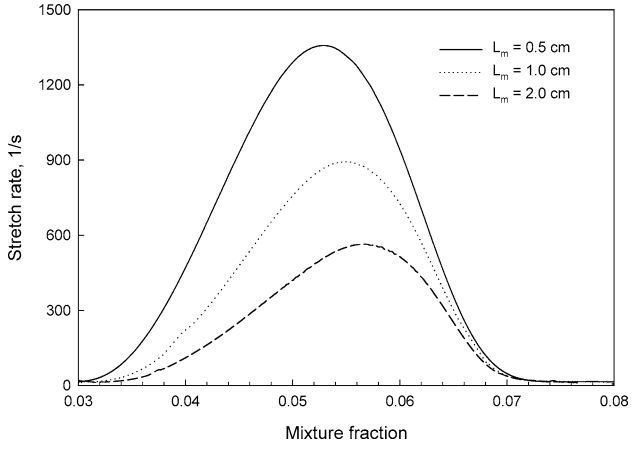

Fig. 7. Stretch rate along the contour line of $X_{CO_2} = 0.043$.

the results obtained from other surfaces, like the contour line of $T = 300$ K, are qualitatively similar.

A triple flame in a mixing layer is strongly stretched, since the flame surface is curved and the fluid flow diverges, as seen in Fig. 2. Fig. 7 shows the stretch rate along the contour line of $X_{CO_2} = 0.043$ for the three triple flames. The stretch rate was calculated as [28]

$$k = -\vec{n}\vec{n} : \nabla\vec{V} + \nabla \cdot \vec{V} + s_d(\nabla \cdot \vec{n}) \tag{7}$$

where $\vec{n}$ is the unit vector normal to the flame surface, s_d is the local flame propagation speed (obtained using the above burning flux divided by density), $\vec{V}$ is the local flow velocity, and $\nabla \cdot \vec{n}$ is the curvature of the flame surface. It is illustrated that the highest stretch rates occur in the near-stoichiometric mixture fraction region. The stretch rate increases with the decrease in mixing layer thickness. For the mixture fractions further off the stoichiometric value, both the magnitude of the stretch rate and the difference in the stretch rate between the three flames decrease. The stretch rate obtained from the contour line of $T = 300$ K is qualitatively similar to that from the contour line of $X_{CO_2} = 0.043$. The stretch rate of a one-dimensional planar premixed flame is zero.

From Figs. 6 and 7, we find that in the near-stoichiometric mixture fraction region, the higher the stretch rate, the lower the burning speed. However, the situation reverses when the mixture fraction is far from the stoichiometric value.

We now examine if the theories of burning speed versus stretch rate established for homogeneous premixed flames can explain the phenomenon observed in triple flames. The results regarding the response of burning speed to stretch for homogeneous methane/air premixed flames in the literature are somewhat inconsistent. A well-known viewpoint [29] suggests that positive stretch enhances the burning intensity of a lean mixture and reduces that of a rich mixture for methane/air premixed flames, due to the Lewis number effect. Conversely, a numerical study by Davis et al. [30] shows that for methane/air premixed flames with equivalence ratios from 0.6 to 1.4, the Markstein number is always greater than zero and thus positive stretch reduces the burning speeds for both lean and rich methane/air mixtures. While it is still hard to justify which of these two viewpoints is correct, we find that neither of them can completely explain the burning speed response to stretch in the triple flames of this paper. The first viewpoint [29] can partially explain the phenomena in triple flames in regions where the mixture fractions are either slightly larger or much lower than the stoichiometric value. However it fails in regions where the mixture fraction is either slightly less or much larger than the stoichiometric value. On the other hand, the viewpoint of Davis et al. [30] can explain the results in the near-stoichiometric mixture fraction region, but fails in the regions with mixture fraction far from stoichiometric value (either lean or rich).

The existing theories of the burning speed response to stretch established from homogeneous premixed flames cannot completely explain the phenomena observed in triple flames. This result is in disagreement with Qin et al. [12], but to a certain extent consistent with Plessing et al. [11].

The principal reason that the response of triple flames to stretch differs from that of homogeneous premixed flames is the interaction between the three branches of a triple flame. The effect of this interaction is particularly significant in the region with mixture fraction far from the stoichiometric value, since the two premixed flame branches are separated by and gradually becoming almost parallel to the diffusion flame branch. Therefore there is heat transfer and radical exchange between the diffusion and the two premixed flames. The direct interaction between the two premixed flame branches can be neglected.

As shown in Fig. 3, the temperature in the diffusion branch of a triple flame is higher than in the two premixed branches. Consequently there is lateral heat transfer from the diffusion branch to the premixed branches. With the decrease of the mixing layer thickness, the space between the diffusion branch and the two premixed branches reduces. Consequently the heat transfer rates from the diffusion branch to the premixed branches are higher, which leads to the higher burning fluxes in the premixed branches of triple flames with narrower mixing layer or higher mixture fraction gradient.

In addition to the lateral heat transfer, the interaction also results from the exchange of radicals between the diffusion and the premixed flames. The radicals formed in the diffusion flame, such as OH and H, diffuse to the two premixed flames, which intensifies the combustion in the premixed flames. This interac-

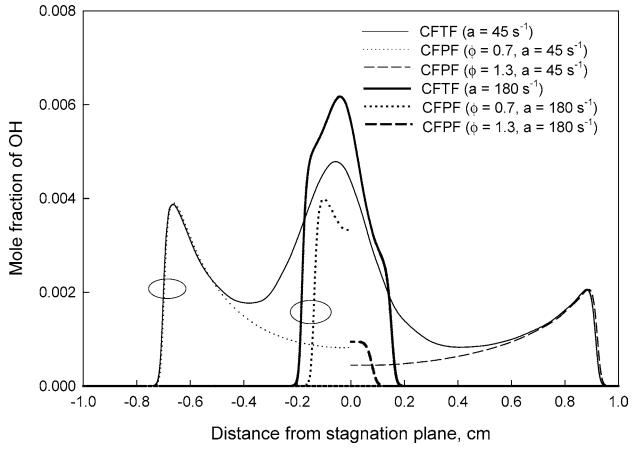

Fig. 8. Mole fraction of OH in two counterflow triple flames (CFTFs) and the corresponding counterflow premixed flames (CFPFs). Quantity a represents stretch rate.

tion is also strengthened with the decrease in the space between the diffusion and the premixed flames. For triple flames with narrower mixing layers, the space between the diffusion and the two premixed flames reduces and thus the interaction is stronger.

Therefore both the heat transfer and radical exchange between the diffusion and premixed branches in a triple flame are enhanced with the decrease of the mixing layer. To clearly show and understand the interaction between the diffusion and premixed branches in triple flames, in addition to the simulations of the previous triple flames in 2-D mixing layers, we also did calculations for axi-symmetric counterflow flames. The simple configuration of counterflow flame not only produces the similar interaction between the diffusion and premixed branches of triple flames, but also allows us to exactly identify how the interaction is caused.

Fig. 8 displays the concentrations of OH in two counterflow triple flames (CFTFs) of different stretch rates and the corresponding counterflow premixed flames (CFPFs). The CFTFs were produced by lean and rich CH_4/air mixtures, respectively, issuing from two opposed nozzles, while the corresponding CFPFs were produced by identical CH_4/air mixtures issuing from the opposed nozzles. The equivalence ratios of the rich and the lean mixtures are, respectively, 1.3 and 0.7. The configurations of CFTF and CFPF are shown in Fig. 9. Note that only halves of the CFPF's profiles are displayed in Fig. 8 due to the symmetry. It is observed that when the stretch rate is 45 s^{-1}, the differences in OH concentrations of the premixed flames of the CFTF and the corresponding CFPFs are negligible. However, with the stretch rate being increased to 180 s^{-1}, the OH concentrations in the premixed flames of the CFTF are significantly higher than in the corresponding CFPFs. This is because the diffusion and the premixed flames of this CFTF are closer owing to the higher stretch rate, and thus the interaction between them is more significant. For triple flames in 2-D mixing layers, the same interaction exists. The interaction is intensified when the mixing layer is narrower due to the higher stretch rate, as shown in Fig. 7.

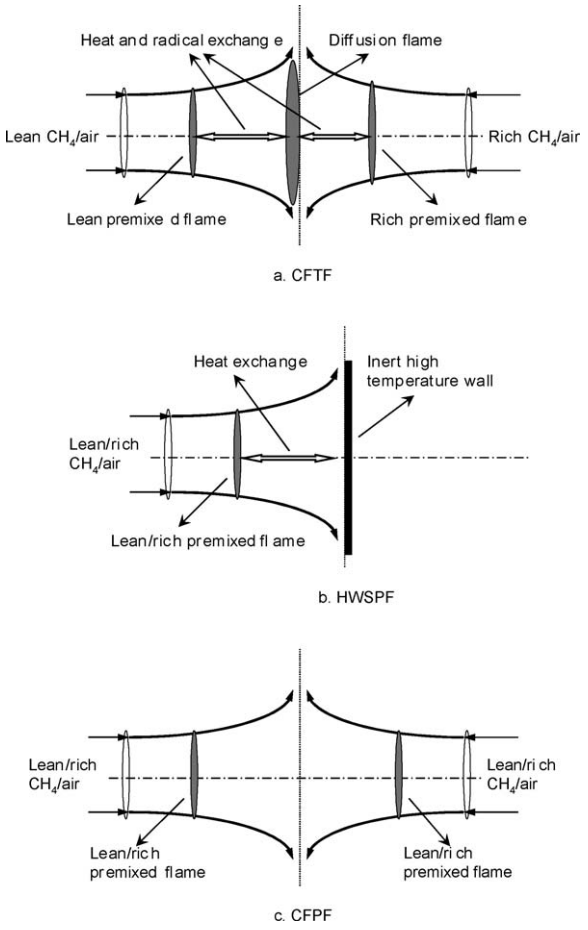

Fig. 9. Schematic configurations of three counterflow flames. (a) CFTF; (b) HWSPF; (c) CFPF.

The heat transfer and the exchange of radicals enhance the local burning velocities in the premixed branches of a triple flame. For a triple flame with narrower mixing layer, the stronger interaction between the diffusion and the premixed flames causes the higher local burning fluxes in the region with mixture fraction far from the stoichiometric value. This successfully explains the results of Figs. 6 and 7 in regions with mixture fractions far off the stoichiometric value, where the narrower the mixing layer, the higher the local burning flux.

To identify the relative importance of the two effects, the heat transfer and the radical exchange, we further examine the results of the above CFTF with the stretch rate of 180 s^{-1} and the corresponding CFPFs. In addition to this CFTF and the corresponding CFPFs, we carried out simulations of two additional stretched premixed flames with the same stretch rate. These two stretched premixed flames were generated by issuing the lean or rich CH_4/air mixture from a nozzle and impinging the jet on an inert high temperature wall. The temperature of the wall was specified as the maximum temperature of the CFTF. We refer to these two extra stretched premixed flames as High Temperature Wall Stabilized Premixed Flames (HWSPFs). The schematic configuration of HWSPF is also shown in Fig. 9. Being different from the rich and lean premixed flame branches of the CFTF, there is no radical exchange between the inert hot wall and the reaction zone for the two HWSPFs. However, because

of the high temperature of the wall, the heat transfer from the wall to the reaction zones exists. Consequently the differences between the two premixed flames of the CFTF and the corresponding lean and rich HWSPFs are due to the radical exchange between the diffusion and two premixed flames in the CFTF. Because of the symmetry, there is neither heat transfer nor radical exchange between the stagnation plane and a lean or rich CFPF. Accordingly the disparities between the HWSPFs and the corresponding CFPFs are caused by the heat transfer from the wall to the reaction zones, which is similar to the heat transfer from the diffusion flame to the premixed flames in the CFTF. Fig. 10 shows the mole fractions of OH and the consumption rates of methane for the CFTF, HWSPFs and the corresponding CFPFs. It is clearly demonstrated that the heat transfer and radical exchange between the diffusion and the premixed flames play similar roles in affecting the local burning characteristics of the premixed branches of a triple flame. For example, the diffusion of OH and the heat transfer from the diffusion flame significantly increases the concentrations of OH in the two premixed flames of the CFTF. As a result, the consumption rates of methane in the two premixed flames of the CFTF are intensified, and the two premixed flames of the CFTF can move further away from the stagnation plane, compared to the corresponding CFPFs.

It should be pointed out that the role of the interaction between the diffusion flame and the premixed flames in affecting the local burning properties is only significant in the region with mixture fractions far from stoichiometric value for triple flames in 2-D mixing layers. When the stoichiometric mixture fraction region is gradually approached from either the lean or rich side, the two premixed flames become almost vertical to the diffusion flame. The heat transfer and radical exchange between the diffusion flame and two premixed flames become negligible. Therefore the effect of the interaction between the diffusion flame and the premixed flames on the local burning velocity almost disappear in the near stoichiometric mixture fraction region. The main factor affecting the local burning velocity in this region should be the stretch, as in a homogeneous premixed flame. Figs. 6 and 7 show that the higher the stretch rate (or the narrower the mixing layer), the lower the local burning velocity is in the near stoichiometric mixture fraction region. This result is consistent with the previous results of other investigators, such as [4,5,14]. It suggests that the Markstein number for near stoichiometric CH_4/air mixtures (either lean or rich) is positive, and thus positive stretch reduces the burning velocity. This supports the conclusion of Davis et al. [30].

3.3. Effect of radiation on local burning flux

The heat transfer from the diffusion branch to the premixed branches in a triple flame can be caused by radiation and conduction. Convection is negligible, since the velocity component along the lateral direction is very small, as shown in Fig. 2. To study the effect of radiation on local burning flux in a triple flame, we carried out two more simulations for the triple flame configured with a mixing layer of 1.0 cm, in addition to the normal simulation by the radiation model (DOM) described in the numerical model section. The radiation reabsorption term was neglected (i.e. optically thin model) in the first extra simulation, while the radiation heat loss term was totally removed (i.e. adiabatic flame) in the second one. The local burning fluxes obtained from the two surfaces examined previously ($X_{CO_2} = 0.043$ and $T = 300$ K) by the three radiation models are illustrated in Fig. 11. It is observed that there is almost no discernable difference among the results from the three

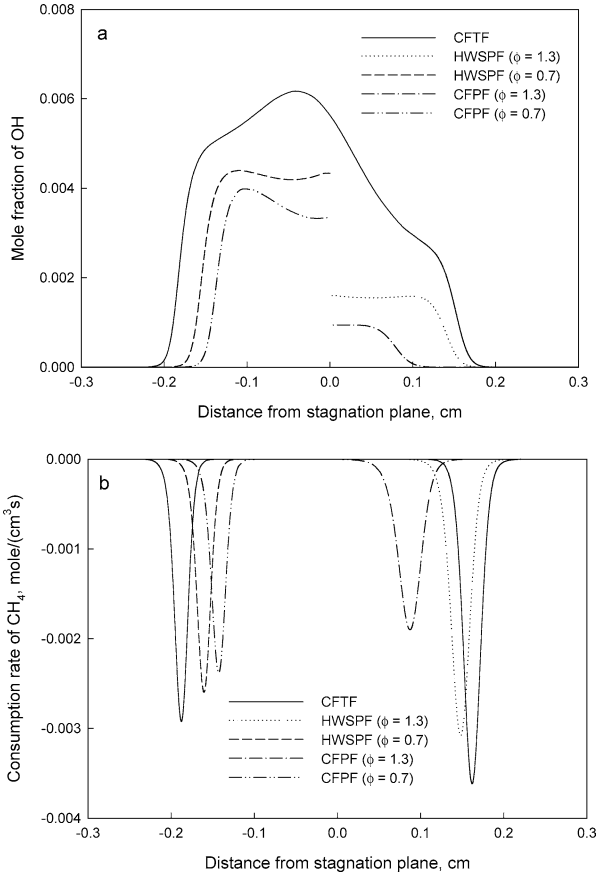

Fig. 10. Profiles of OH mole fractions and CH_4 consumption rates in CFTF, HWSPFs and CFPFs with stretch rate of 180 s^{-1}.

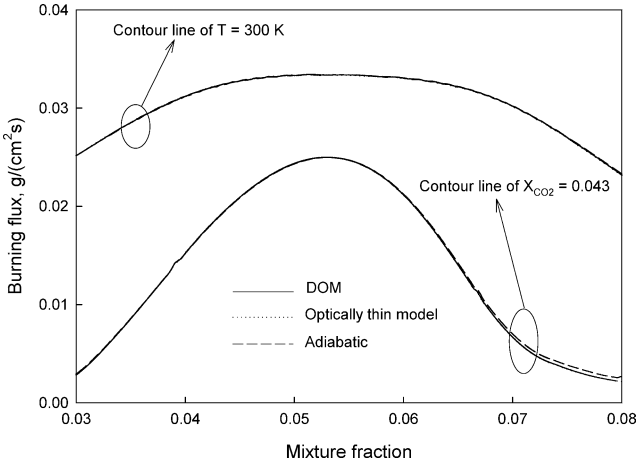

Fig. 11. Burning fluxes of the flame with $L_m = 1.0$ cm from three different radiation models.

radiation models. This implies that radiation is not a significant factor causing the heat transfer from the diffusion to the premixed flame branches and the enhancement of local burning velocity in the premixed flame branches. It may be because flame size is small. Therefore the heat transfer from the diffusion flame branch to the premixed flame branches in a triple flame is mainly caused by conduction.

4. Conclusions

The triple flames in two-dimensional methane/air mixing layers with three different mixture fraction gradients have been numerically investigated. The results indicate that the heat release rate in the diffusion flame branch of a triple flame is much lower than in the two premixed flame branches. With the decrease of the mixing layer thickness, the combustion intensity in the diffusion flame branch of a triple flame is increased. In the near-stoichiometric mixture fraction region, the local burning flux of a triple flame is lower when the mixing layer is narrower. However when the mixture fraction is far from the stoichiometric value, the local burning flux is increased as the mixing layer thickness is reduced. The correlation of burning speed versus stretch rate from homogeneous premixed flames cannot completely explain the phenomenon in a triple flame. This is due to the interaction between the diffusion and the premixed flame branches, which significantly affects the local burning velocity in the region with mixture fraction far from the stoichiometric value in a triple flame. This interaction is caused by conduction heat transfer and radical exchange between the diffusion flame branch and premixed flame branches. Radiation has negligible effect on local burning properties of a triple flame.

References

[1] H. Phillips, Flame in a buoyant methane layer, in: Proceedings of Tenth Symposium (Int.) on Combustion, The Combustion Institute, 1965, pp. 1277–1283.
[2] A. Liñán, A. Crespo, An asymptotic analysis of unsteady diffusion flames for large activation energies, Combust. Sci. Technol. 14 (1976) 95–117.
[3] J.W. Dold, Flame propagation in a nonuniform mixture: analysis of a slowly varying triple flame, Combust. Flame 76 (1989) 71–88.
[4] P.N. Kĩoni, B. Rogg, K.N.C. Bray, A. Liñán, Flame spread in laminar mixing layers: the triple flame, Combust. Flame 94 (1993) 276–290.
[5] G.R. Ruetsch, L. Vervisch, A. Liñán, Effects of heat release on triple flames, Phys. Fluids 7 (1995) 1447–1454.
[6] J. Boulanger, L. Vervisch, J. Reveillon, S. Ghosal, Effects of heat release in laminar diffusion flames lifted on round jets, Combust. Flame 134 (2003) 355–368.
[7] T. Echekki, J.H. Chen, Structure and propagation of methanol–air flames, Combust. Flame 114 (1998) 231–245.
[8] P.N. Kĩoni, K.N.C. Bray, Greenhalgh, B. Rogg, Experimental and numerical studies of a triple flame, Combust. Flame 116 (1999) 192–206.
[9] J. Buckmaster, M. Matalon, Anomalous Lewis number effects in tribrachial flames, in: Proceedings of Twenty-Second Symposium (Int.) on Combustion, The Combustion Institute, 1988, pp. 1527–1535.
[10] R. Azzoni, S. Ratti, I.K. Puri, S.K. Aggarwal, Gravity effects on triple flames: flame structure and flow instability, Phys. Fluids 11 (1999) 3449–3464.
[11] T. Plessing, P. Terhoeven, N. Peters, M.S. Mansour, An experimental and numerical study of a laminar triple flame, Combust. Flame 115 (1998) 335–353.
[12] X. Qin, I.K. Puri, S.K. Aggarwal, Characteristics of lifted triple flames stabilized in the near field of a partially premixed axisymmetric jet, Proc. Combust. Inst. 29 (2002) 1565–1572.
[13] H.G. Im, J.H. Chen, Structure and propagation of triple flames in partially premixed hydrogen–air mixtures, Combust. Flame 119 (1999) 436–454.
[14] H.G. Im, J.H. Chen, Effects of flow strain on triple flame propagation, Combust. Flame 126 (2001) 1384–1392.
[15] R.D. Lockett, B. Boulanger, S.C. Harding, D.A. Greenhalgh, The structure and stability of the laminar counter-flow partially premixed methane/air triple flame, Combust. Flame 119 (1999) 109–120.
[16] Y.S. Ko, S.H. Chung, Propagation of unsteady tribrachial flames in laminar non-premixed jets, Combust. Flame 118 (1999) 151–163.
[17] J. Lee, S.H. Won, S.H. Jin, S.H. Chung, O. Fujita, K. Ito, Propagation speed of tribrachial (triple) flame of propane in laminar jets under normal and micro gravity conditions, Combust. Flame 134 (2003) 411–420.
[18] V.S. Santoro, A. Liñán, A. Gomez, Propagation of edge flames in counterflow mixing layers: experiments and theory, Proc. Combust. Inst. 28 (2000) 2039–2046.
[19] C.E. Frouzakis, A.G. Tomboulides, J. Lee, K. Boulouchos, From diffusion to premixed flames in an H_2/air opposed-jet burner: the role of edge flames, Combust. Flame 130 (2002) 171–184.
[20] K.K. Kuo, Principles of Combustion, John Wiley & Sons, New York, 1993.
[21] F. Liu, G.J. Smallwood, Ö.L. Gülder, Band lumping strategy for radiation heat transfer calculations using a narrowband model, J. Thermophys. Heat Transfer 14 (2000) 278–281.
[22] R.J. Kee, G. Dixon-Lewis, J. Warnatz, M.E. Coltrin, J.A. Miller, A Fortran computer code package for the evaluation of gas-phase, multicomponent transport properties, Report No. SAND 86-8246, Sandia National Laboratories, 1986.
[23] S.V. Patankar, Numerical Heat Transfer and Fluid Flow, Hemisphere, New York, 1980.
[24] Z. Liu, C. Liao, C. Liu, S. McCormick, Multigrid method for multi-step finite rate combustion, Paper No. AIAA 95-0205, 1995.
[25] G.P. Smith, D.M. Golden, M. Frenklach, N.W. Moriarty, B. Eiteneer, M. Goldenberg, R.K. Bowman, C.T. Hanson, S. Song, W.C. Gardiner, J.V.V. Lissianski, Z. Qin, 1999; http://www.me.berkeley.edu/gri_mech/.
[26] R.J. Kee, J.A. Miller, T.H. Jefferson, A General-Purpose, Problem-Independent, Transportable, Fortran Chemical Kinetics Code Package, Report No. SAND 80-8003, Sandia national Laboratories, 1980.
[27] R.W. Bilger, The structure of turbulent nonpremixed flames, in: Proceedings of Twenty-Second Symposium (Int.) on Combustion, The Combustion Institute, 1988, pp. 475–488.
[28] T. Poinsot, D. Veynante, Theoretical and Numerical Combustion, R.T. Edwards, Philadelphia, PA, 2001.
[29] C.K. Law, C.J. Sung, Structure, aerodynamics, and geometry of premixed flamelets, Progr. Energy Combust. Sci. 26 (2000) 459–505.
[30] S.G. Davis, J. Quinard, G. Searby, Determination of Markstein number in counterflow premixed flames, Combust. Flame 130 (2002) 123–136.